AUTOMATIC RECOGNITION OF DENTAL PATHOLOGIES AS PART OF A CLINICAL DECISION SUPPORT PLATFORM

Marin, Iuliana; Goga, Nicolae; Vasilateanu, Andrei; Pavaloiu, Ionel-Bujorel

Génie biomédicale

AUTOMATIC RECOGNITION OF DENTAL PATHOLOGIES AS PART OF A CLINICAL DECISION SUPPORT PLATFORM

IULIANA MARIN[1], NICOLAE GOGA[1,2], ANDREI VASILATEANU[1], IONEL-BUJOREL PAVALOIU[1]

Key words: Dental scan, Automatic pathologies recognition, Digital imaging and communications in medicine (DICOM).

The current work is done within the context of Romanian National Program II (PNII) research project "Application for Using Image Data Mining and 3D Modeling in Dental Screening" (AIMMS). The AIMMS project aims to design a program that can detect anatomical information and possible pathological formations from a collection of digital imaging and communications in medicine (DICOM) images. The main function of the AIMMS platform is to provide the user with the opportunity to use an integrated dental support platform, using image processing techniques and 3D modeling. From the literature review, it can be found that for the detection and classification of teeth and dental pathologies existing studies are in their infancy. Therefore, the work reported in this article makes a scientific contribution in this field. In this article it is presented the relevant literature review and algorithms that were created for detection of dental pathologies in the context of research project AIMMS.

1. INTRODUCTION

The AIMMS project (http://**aimms**.**osf**-demo.com/) intends to design a program that can detect anatomical information and possible pathological structures from a collection of digital imaging and communications in medicine (DICOM) images. The main function of the AIMMS platform is to provide the user with the opportunity to use an integrated dental support platform, using image processing techniques and 3D modeling. From the literature review, it can be found that on the direction of detection and classification of teeth and dental pathologies existing studies are in their infancy. Therefore, the work reported in this article makes a scientific contribution in this field. In this article we present relevant literature review and algorithms that were created for detection of dental pathologies in the context of research project AIMMS.

Cone beam computed tomography (CBCT) provides data as a sequence of cross sections of the body, stored as DICOM images. Despite the much lower exposure to radiation, the results are nowadays comparable to standard CT [1]. In order to reconstruct the 3D structure from the DICOM, the following operations must be performed: image preprocessing, contour detection, segmentation, recording, and ultimately 3D reconstruction [2‒4].

CBCT images are of relatively low quality due to the low radiation dose used, being characterized by a relatively high noise level and low contrast. To these, the artifacts given by the metal inserts due to the tomographic process are added.

First, image filtering is required to eliminate noise and to smooth. Some 2D filters that can be used are Gaussian and medium filters. CBCT offers rather noisy images, so filtering is a necessary step to go further.

In a CT section, contours mainly correspond to boundaries of different entities, such as teeth, bones, flesh, implants, etc. Contours can be detected using Canny filters or variations of them. Contours correspond to the gradient of the image so that a threshold will be used to select the desired margins. Because of the blur of images, the threshold can be an adaptive one, including the hysteresis threshold. Thinning can be used to eliminate unwanted fake spots on the edges. High quality contours are required because they are used for segmentation as well as for registration.

The knowledge about the 3D shape and the structure of each tooth, the arrangement of the teeth to each other and the location of the roots in the jaw and jaw is essential in a lot of maxillofacial surgical procedures, endodontic procedures and treatment simulations [5‒8]. The 3D model is an important component for the simulation of maxillofacial surgery and for treatment.

The next section introduces the state of art regarding dental image processing and pathologies detection. In Section 3 are described the methods used for pathologies detection and in Section 4 results of the research are exposed. The conclusions are presented in the last section.

2. STATE OF ART

Many computers assisted procedures for dentistry applications are based on automatic segmentation and volumetric visualization of teeth.

2.1. SEGMENTATION

Several authors reported different techniques for teeth segmentation in dental radiography, with panoramic, peripheral and biting images. A semi-automatic extraction method of the tooth contour based on the integral projection and the Gaussian blend pattern was proposed in [9]. The approach of [10] was based on the application of morphological operators and adaptive thresholds to separate each tooth from its surroundings.

In [11], the use of iterative thresholds, followed by the use of adaptive thresholds, is used to segment the teeth and separate the background. The watershed algorithm was used in [12] to find the orthodontic features of the teeth in the 3D profile of dental images on dental impressions. In [13], a method based on pulse coupled neural networks performs segmentation of teeth and other bone tissues using an adaptive threshold method. In [14], segmentation uses active contours for radiographies with low contrast. In [15], the contour of the teeth was extracted by using active contours with patterns using the directional gradient.

The active edgeless border was used in [16] to track the contour of the teeth. In [17, 18], a segmentation technique using variable-level sets was used for digital radiography

analysis. A model based on pathological modeling, principal component analysis and support vector machine were presented in [19] for teeth segmentation.

Segmentation of dental images, especially volumetric using CBCT, has been poorly studied. An image segmentation algorithm based on B-spline curves for creating smooth CT regions of the tooth was proposed in [20]. The algorithm prevents the B-spline algorithm from matching mistakes by providing precise tooth initials in the representation process. This technique proposed an optimum threshold scheme using the intensity and shape information obtained from the previous section to generate the original boundaries and an efficient matching method with B-spline functions based on genetic algorithms.

In [21], the teeth were segmented in an interactive manner based on the curve values of the triangle network. These characteristic points are linked to feature regions to extract the characteristic lines in these regions. Therefore, the characteristic outline can be obtained with the help of user information.

In [22] a semi-automatic strategy was introduced for drawing dental contours from dental CT images. A CT section is selected and the interactive teeth segmentation uses the known shape of each tooth.

Dental CT images have the following distinct features: in two adjacent CT sections, the size, location and intensity of a tooth is very similar, so that the tooth framing box whose contour has been drawn corresponds to that region on the next section. Then, the segmentation operation can be performed with a tooth in the given region using the region growth algorithm and the information obtained from the previous section. With the reference section chosen as the starting section, teeth segmentation is performed sequentially automatically.

In the segmentation phase, the manual operation is not only a time consuming and tedious, but often an inaccurate process. Segmentation by experts is variable up to 20 % [23]. Also, conventional approaches, such as the use of exhaustive thresholds, which are used in most 3D reconstruction systems, are not suitable for tooth segmentation in CT images. Therefore, it is necessary to use automated seg-mentation methods that require less interaction with the user [24–27].

2.2. RECONSTRUCTION OF 3D IMAGES

Once the preprocessing and segmentation of 3D images has been done, the next step is the 3D reconstruction of the teeth. Detecting 3D elements in a picture, an important problem in many systems [28] is hard to solve for biological images [29].

3D reconstruction offers many advantages for doctors by allowing them to use large volumes of data and to observe the patient's evolution from one examination to the next. Generally, for 3D reconstruction the steps are as follows: the image is filtered to remove noise and smooth; Segment the image (using, for example, the Mean-Shift segmentation algorithm) and the edges are extracted using, for example, the Canny detector; for each segment, the corresponding associated points are searched (using, for example, the SURF-SSD method).

The mean-shift segmentation algorithm [30–32] aggregates an n-dimensional dataset associating each point with a peak of probability density. The peak is calculated by defining a spherical window r and calculating the average of the points in that window. The algorithm then moves the window to the average and repeats until convergence.

Feature matching algorithms work by extracting important features in the 3D scene (borders, contours) [33] and then a 3D model is created by matching the key points of the features. There are several matching algorithms such as correlation, normalized correlation, sum of square gap and sum of absolute difference [34].

The purpose of speeded-up robust features (SURF) is to encode distinctive local structures for image matching despite small changes in viewing conditions (scaling, orientation, and contrast). SURF is a variant of the SIFT (Scale-Invariant Feature Transform) algorithm. SURF uses the entire image to generate key points and descriptors. SIFT creates image pyramids, filtering each layer with Gaussian filters with increasing sigma values and making the difference. SURF builds a stack of images with equal resolution [35].

2.3. DETECTION AND CLASSIFICATION OF TEETH AND DENTAL PATHOLOGIES

Once the 3D image has been reconstructed, the next step is the detection and classification of teeth and dental pathologies. Although there are algorithms for tooth classification, classification of dental pathologies is an open research field to be addressed.

Research on maxillary segmentation in CT focused mainly on the lower jaw [36–39], because the upper jaw is generally more difficult to segment automatically. The upper jaw has thin bone structures (mouth of the mouth, maxillary sinus, orbital walls), which are hard to detect only on the intensity thresholds [40–41].

There have been several attempts such as Kainmueller and colab. [42] that segments the maxillary bone of the front face. However, tooth regions are omitted in most studies due to the aforementioned artifacts. The problem of teeth detection in medical imaging has been well studied for 2D, but poorly researched for 3D imagery, because the effects of metallic artifacts are less severe in 2D than in 3D.

Mahoor and colab. [43], Nassar and colab. [44] and Lin and colab. [45] isolate a tooth from the row of the teeth, classify separately every isolated tooth and adjust the results. For this, integral teeth projection is used. Then each region of an isolated tooth is classified based on the characteristics of the area [44] or the shape characteristics [43, 45]. The last one needs a segmentation of each tooth belonging to the isolated region. After the separate classification of each region, the result is adjusted according to the order of the teeth. At this stage, alignment techniques are used.

Gao and colab. [46] and Hosntalab and colab. [47] propose segmentation algorithms for 3D imagery CT. Unfortunately; a teeth classification is not done. The needed input is the segmentation of the tooth region.

The first pathologies that can be classified are the presence and absence of teeth. More advanced research for other dental pathologies is relatively rare in the early stages, this being one of the scientific contributions of the work presented in this paper.

Once the teeth have been classified and part of the dental pathologies, the next step would be the computerized help

of medical diagnostics. However, there is not much literature on the medical diagnosis of dental pathologies, this being a contribution that will be brought by the work presented in this article.

In this section, an analysis of relevant literature has been made on several directions, representing the steps of processing dental data CTs.

These are:

- Preprocessing 3D images (segmentation);
- Reconstruction of 3D images;
- Computerized medical diagnosis.

From the analysis of the existing literature and from the previous work, it was found that for the first two stages (preprocessing and eventually reconstruction of 3D images) the algorithms are relatively well defined although there is room for improvement [48–52, 55]. At the third stage (medical diagnosis, including classification of existing teeth and their status), for the recognition of dental pathologies, existing studies are in their infancy, the work reported in this article having the role of making a scientific contribution especially in this field [53, 54, 56].

3. DETECTION OF PATHOLOGIES

For a teeth detection algorithm the steps that were followed are the following. First, a precise and robust segmentation of the structure [42] and then a 3D reconstruction is achieved. Then, this segmentation will be used to detect the tooth regions (for example by identifying 15 separation planes). After which, every region will be classified as "tooth" or "missing" to obtain the state of individual teeth.

3.1. EDENTATION

The DICOM data consists of several tens of slices with the usual thickness of 1mm, each with the size of 512×512 pixels. Adaptive threshold segmentation is used to detect the teeth and contours are extracted. The method is exposed to errors because of the variations in intensity, so it is complemented with Canny edge detection, where the pixels which have large gradients or just average ones but are connected to the prior ones will be contour points [48, 49].

The CT is analyzed in order to identify if it corresponds to the mandible or to the maxilla. For a mandible, the blueprint of the teeth is more visible than for the maxilla. The smaller contrast will give a smaller number of clear contour points, which can be used to validate the region, beside the recognition of the anatomical features.

The segmentation of the teeth begins from the crown section where the best contrast is found. The contours in consecutive slices are barely changing, excepting the cases of roots or splits. Several sections are associated to the same object/tooth when the center of each section is placed inside the contour of the object in the next section closer to the crown. If the angular distance between the centers of consecutive teeth is greater than a statistical limits, missing tooth are reported [52]. The teeth delimitation for the mandible scan is illustrated in Fig. 1.
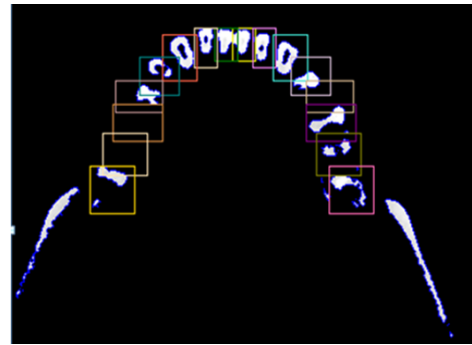

Fig. 1 – Teeth delimitation.

3.2. CAVITIES

The cavities detection was performed by firstly determining the coordinates of the contour center of gravity.

The coordinates of the contour center of gravity of the analyzed tooth is determined using the sum of all the remaining blue pixel coordinates, which is divided by the total number of pixels found.

The first point that belongs to the contour of the current being examined is determined to be placed on the left side of the center of gravity or on the right side of it. If none of these points is found, then the search is done above or below the center of gravity.

The rest of the points are found by considering that the tooth is divided into four parts or quadrants and the search for the successive points that belong to the contour is determined by a possible orientation.

Starting with the point taken as reference, the coordinates X and Y change according to the orientation of the next point that belongs to the contour of that tooth.

Regardless of the position of the first point placed on the contour, the successive point is selected so that the pixel belongs to the same or next quadrant. The next point is determined according to the quadrant to which the current point belongs.

If the current point is placed in the first quadrant, with X and Y coordinates smaller than the center of gravity, then the possible directions are West, North-West, North, North-East, East and South-East, including dental cavities, as in the figure below where they are illustrated using thick arrows.
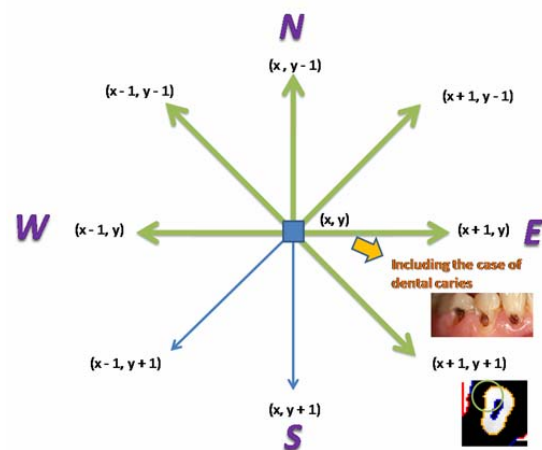

Fig. 2 – Finding the next point, the current point being placed in the first quadrant.

When traveling in the South-East direction, the points that have been visited from northwest direction should not be returned. By considering the point X_1 before X_2 and X_3, two cases are illustrated in Figs. 3 and 4.
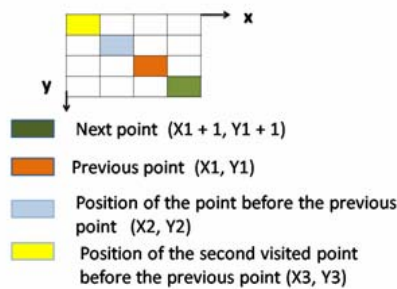

Fig. 3 – Find the next point where the previous points respect the following condition $X_2 < X_1$ and $Y_2 <= Y_1$ [50].
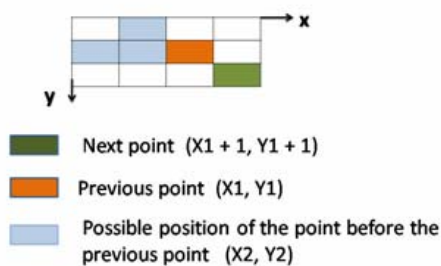

Fig. 4 – Find the next point where the preceding points respect the following condition $X_3 < X_2 < X_1$ and $Y_3 > Y_2 > Y_1$.

If the last point is placed in quadrant 1, but it does not find any correspondent, then the rightmost point in the first quadrant must be found, if it exists, and draw a line using Bresenham's algorithm to unite them. The other case is when if a point in the quadrant 1 has no point in the neighborhood, the leftmost point in the quadrant 2 is selected and a line is drawn between the two points using Bresenham's algorithm.

In addition, when teeth are very close, they must be separated by drawing a line using Bresenham's algorithm. For the remaining quadrants, this procedure to find a corresponding point is repeated, the search direction being changed. If the current point is placed in the second quadrant, the possible directions are North-East, East, South-East, South and South-West. If the current point is placed in the third quadrant, the possible directions are North, South-East, South, South-West and West. If the current point is placed in the fourth quadrant, the possible directions are North, North-East, North-West, West, South-West and South.

If there is an angle of 90^0 in a neighborhood of eight consecutive points, there is a cavity in that region. The angle is calculated using the cosine theorem, where a, b and c are the sides of the triangle.

An example of cavities that were detected using the previous described method is illustrated in Fig. 5.
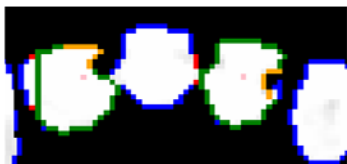

Fig. 5 – Cavities detection for incisors 31 and 42.

3.3. PERIODONTITIS

The teeth appear just in a specific range of CT slides. Periodontitis is found by filtering the coronal planes from the specified range according to a color intensity threshold. All the pixels below this value are transformed into black pixels.

As for the cavities, the neighboring pixels between the detected pixels are the ones which turned black are colored differently. These pixels appear blue in the Bitmap image. In the algorithm, the first step which was done was for edentation, this being described in the previous paragraph. During the edentation step, it was discovered whether the DICOM belongs to the mandible or to the maxilla of the patient. If the DICOM belongs to the maxilla, then the image is rotated with 180^0 degrees and it is prepared for the detection of periodontitis.

Periodontitis is a gum infection that leads to the creation of plaque and calculus that destroys the enamel and weaken the healthy bone level and to inflammation.

This inflammation affects the soft tissue and ruins the bone which supports the tooth, creating a space between the gum and the tooth. The space can be detected on the DICOM CT slices.

For example, for the mandible of a patient, the presence of periodontitis at the molar 38 can be observed in Fig. 6 in the region delimited by the circle.
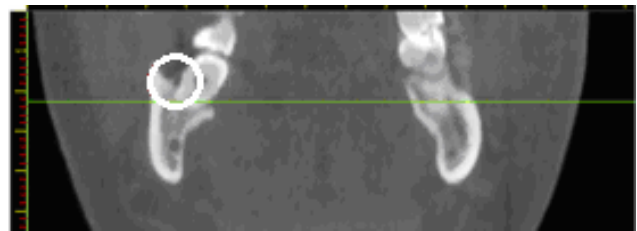

Fig. 6 – Presence of periodontitis in a given CT DICOM.

In order to detect the space between the gum and the tooth, the left and right side contours of each coronal plane from the range of interest need to be determined. For this, the top left most, top right most, bottom left most and bottom right most points of coordinates X and Y are found.

The left side contour is found by using a bottom to top search in the directions North, North-West, North-East, East, West, South-East and South, each point being able to be visited just once.

The right side contour is found by using a bottom to top search in the directions North, North-West, North-East, East, West, South-West and South, each point being able to be visited just once.

The presence of periodontitis for each of the contours is found by seeing that the pattern is similar to a convex function (which holds water). For this, the equation $ax^2 + bx + c = y$, formed by three points belonging to the contour needs to be found.

The unknowns a, b, c can be found by inserting the points (x_1, y_1), (x_2, y_2), (x_3, y_3) in the previous equation:

$$\begin{cases} y_1 = ax_1^2 + bx_1 + c \\ y_2 = ax_2^2 + bx_2 + c. \\ y_3 = ax_3^2 + bx_3 + c \end{cases} \qquad (1)$$
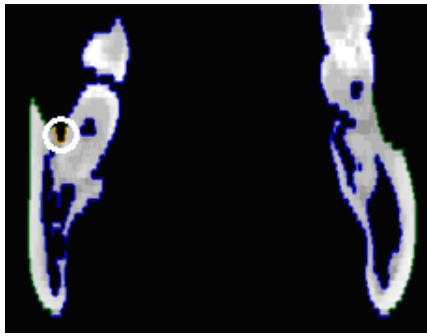
Fig. 7 – Presence of periodontitis.

The system can be solved numerically or one can determine the relations for *a, b, c*. The solution for *a* is:

$$a = \frac{x_1(y_2 - y_3) + x_2(y_3 - y_1) + x_3(y_1 - y_2)}{(x_1 - x_2)(x_2 - x_3)(x_3 - x_1)} \qquad (2)$$

The sign of the function is set using the second derivative which depends on the sign of *a*. If the sign is positive, the function is convex, else the function is concave.

For the general case, the system of coordinates is rotated such that the Ox axis is parallel to the teeth line, pointing to the exterior. An alternative method is to compute the second derivative for the chaincode of pixels belonging to the contour.

It should also be taken under consideration that the angle between the points should have the value between 60° and 90°, using the dental medicine specialists opinion.

In Fig. 7 can be seen the contours from the left and right side, as well the detection of periodontitis. The affected region is delimited by a circle.

The tooth is detected using the slide number that corresponds to the *y* coordinate of the teeth from the transversal view, so that the teeth positions determined in the first paragraph are also used here. The program announces which are the slides where periodontitis was initially found, after which the results are refined, based that for periodontitis to exist, it should appear on three successive slides.

The tooth from Fig. 7 is the one which presented the illness in Fig. 5. Based on it, the program affirms initially that it found several planes with periodontitis but after refining the results based on the successive appearance of the illness on three slides, the program informed that the molar 38 presents periodontitis**.**

4. VALIDATION OF RESULTS

In what follows we present the validation of our results in a set of DICOM dental images.

4.1. EDENTATION VALIDATION

The edentation detection was performed on the mandibles and maxillae of 14 scans, using their DICOM file.

Generally, the algorithm efficiency is of 88 % for the mandible, while for the maxillae the efficiency is around 78 %. As it was stated in the research on maxillary segmentation in CT focused mainly on the lower jaw [53–55] the results were better than for the maxillae. In over 60 % of cases the algorithm used manages to determine all missing teeth. Due to existing artifacts such as poor contrast or tooth movement, there have been some false findings.

4.2. PERIODONTITIS VALIDATION

Periodontitis was detected on the mandibles and maxillae of 8 scans, using their DICOM file.

Generally, the algorithm efficiency is around 80 %. Due to the closeness of molars between the mandible and the maxilla, appears a convex function formed by the points and it notifies the slide to present edentation. The poor contrast also leads to false findings.

For some of the patients the teeth from the maxilla were all missing, so periodontitis could not have been detected.

5. CONCLUSIONS

In this paper we reported a work within the context of the Romanian national project PNII AIMMS for detection of dental pathologies from dental scans.

Generally, we found out that the edentation algorithm efficiency is of 88 % for the mandible, while for the maxillae the efficiency is around 78 %. Due to existing artifacts such as poor contrast or shifting teeth, there were some false detections. Generally, the periodontitis algorithm efficiency is around 80 %.

The work presented in this paper can be used by dentists in their diagnosis work. Further work is related to find new pathologies and try the described algorithms in a larger DICOM set of data and improve it according to the obtained results.

REFERENCES

1. J. Van Dessel et al. *Accuracy and reliability of different cone beam computed tomography (CBCT) devices for structural analysis of alveolar bone in comparison with multislice CT and micro-CT*, Eur J Oral Implantol. **10**, *1*, pp. 95–105, 2017.
2. M. Abdel-Mottaleb, O. Nomir, D. E. Nassar, G. Fahmy, H. H. Ammar, *Challenges of Developing an Automated Dental Identification System*, Circuits and Systems, IEEE 46th Midwest Symposium, 2003.
3. E. Cheng, J. Chen, J. Yang, H. Deng, Y. Wu, V. Megalooikonomou, B. Gable, H. Ling, *Automatic Dent-landmark detection in 3-D CBCT dental volumes*, Conf. Proc IEEE Eng. Med. Biol. Soc., 2011.
4. P. Kamencay, M. Zachariasova, R. Hudec, M. Benco, R. Radil, *3D Image Reconstruction from 2D CT Slices*, 3DTV-Conference: The True Vision – Capture, Transmission and Display of 3D Video (3DTV-CON), 2014.
5. R. Cucchiara, E. Lamma, T. Sansoni, *An image analysis approach for automatically re-orienteering CT images for dental implants*, Comput. Med. Imaging Graph., 2004, pp. 185–201.
6. D. Bossard, N. Dubos, F. Trunde, A. Huet, J.L. Coudert , *3D computed-assisted surgery in orthodontic treatment of impacted canines in palatal position*, Int. Congr. Ser., 2004, pp. 1203–1208.
7. H. Hassan, A. El-Baz, A.A. Farag, A.G. Farman, D. Tasman, W.M. Miller, *A volumetric 3D model of the human jaw*, Int. Congr. Ser., 2005, pp. 1244–1249.

8. F. Pongrdcz, Z. Bdrdosi, *Dentition planning with image-based occlusion analysis*, Int. J. CARS, 2006, pp. 149–156.

9. A.K. Jain, H. Chen, *Matching of dental X-ray images for human identification*, Pattern Recognit., 2004, pp. 1519–1532.

10. J. Zhou, M. Abdel-Mottaleb, *A content-based system for human identification based on bitewing dental X-ray images*, Pattern Recognit., 2005, pp. 2132–2142.

11. O. Nomir, M. Abdel-Mottaleb, *A system for human identification from X-ray dental radiographs*, Pattern Recognit., 2005, pp. 1295–1305.

12. Marielle Mokhtari, D. Laurendeau, *Feature detection on 3D images of dental imprints*, Proc.Workshop on Biomedical Image Analysis, 1994, pp. 287–296.

13. J. Johnson, M. Padgett, *PCNN models and application*, IEEE Trans. Neural Netw., 1999, pp. 480–498.

14. M. Piotrowski, P.S. Szczepaniak, *Active contour based segmentation of low-contrast medical images*, Proc. 1st Int. Conf. on Advances in Medical Signal and Information Processing, 2000, pp. 104–109.

15. H. Chen, A.K. Jain, *Tooth contour extraction for matching dental radiographs*, Proc. 17th Int. Conf. on Pattern Recognition, 2004, pp. 522–525.

16. S. Shah, A. Abaza, A. Ross, H. Ammar, *Automatic tooth segmentation using active contour without edges*, Proc. Biometric Consortium Conference, 2006, pp. 1–6.

17. S. Li, T. Fevens, A. Krzyzak, S. Li, *An automatic variational level set segmentation framework for computer aided dental X-ray analysis in clinical environments*, Comput. Med. Imaging Graph., 2006, pp. 65–74.

18. S. Li, T. Fevens, A. Krzyzak, S. Li, *Semi-automatic computer aided lesion detection in dental X-ray using variational level set*, Pattern Recognit., 2006, pp. 2861–2873.

19. S. Li, T. Fevens, A. Krzyzak, S. Li, *Automatic clinical image segmentation using pathological modeling, PCA and SVM*, Eng. App. Artif. Intell., 2006, pp. 403–410.

20. H. Heo, O. Chae, *Segmentation of tooth in CT images for 3D reconstruction of teeth*, Proc. SPIE, 2004, pp. 455–466.

21. M. Zhao, L. Ma, W. Tan, D. Nie, *Interactive tooth segmentation of dental models*, Proc. 27th Int. Conf. of the Engineering in Medicine and Biology Society, 2005, pp. 654–657.

22. F. Zhang, Y. Fan, F. Pu, Z. Liu, *A semi-automatic method for tooth segmentation in dental CT images*, Chinese J. Biomedical Eng., 2007, pp. 15–18.

23. S. Warfield, J. Dengler, J. Zaers, C. Guttmann, W. Gil, G. Ettinger, J. Hiller, R. Kikinis, *Automatic identification of grey matter structures from MRI to improve the segmentation of white matter lesions*, J. Image Guid. Surg., 1995, pp. 326–338.

24. Sh. Keyhaninejad, R.A. Zoroofi, S.K. Setarehdan, G. Shirani, *Automated segmentation of teeth in multislice CT images*, Proc. Int. Conf. Visual information Engineering, 2006, pp. 339–344.

25. N.T. Duy, H. Lamecker, D. Kainmueller, S. Zachow, *Automatic Detection and Classification of Teeth in CT Data*, Med Image Comput Assist Interv., 2012, pp. 609–616.

26. H.-T. Yau, T.-J. Yang, Y.-C. Chen, *Tooth Model Reconstruction Based upon Data Fusion for Orthodontic Treatment Simulation*, Computers in Biology and Medicine, 2014, pp. 8–16.

27. A.E. Rad, M.S.M. Rahim, A. Norouzi, *Digital Dental X-Ray Image Segmentation and Feature Extraction*, Telkomnika, 2013, pp. 3109–3114.

28. Y. Huang, Z. Qiu, Z. Song, *3D reconstruction and visualization from 2D CT images*, IT in Medicine and Education, 2011, pp. 153–157.

29. J.S. Athertya, S. Poonguzhali, *3D CT image reconstruction of the vertebral column*, Recent Trends in Information Technology, 2012, pp. 81–84.

30. J. Sirotkovic, H. Dujmic, V. Papic, *Accelerating mean shift image segmentation with IFGT on massively parallel GPU*, Information & Communication Technology Electronics & Microelectronics, 2013, pp. 279–285.

31. Q. Mahmood, A. Chodorowski, A. Mehnert, M. Persson, *A novel Bayesian approach to adaptive mean shift segmentation of brain images*, Computer-Based Medical Systems, 2012, pp. 1–6.

32. D. Comaniu, P. Meer, *Robust Analysis of Feature Spaces: Color Image Segmentation*, Proc. IEEE Conf. Computer Vision and Pattern Recognition, 1997, pp. 750–755.

33. A.V. Paramkusam, V.S.K. Reddy, *An efficient fast full search block matching algorithm with SSD criterion*, India Conference (INDICON), 2011, pp. 1–6.

34. R.B. Porter, N.W. Bergmann, *A generic implementation framework for FPGA based stereo matching*, Proceedings of IEEE, Speech and Image Technologies for Computing and Telecommunications, 1997, pp. 461–464.

35. H. Bay, A. Ess, T. Tuytelaars, L.V. Gool, *Speeded-Up Robust Features*, Computer Vision and Image Understanding, 2008, pp. 346–359.

36. M. Lilja, V. Vuorio, K. Antila, H. Setal, J. Jarnstedt, M. Pollari, *Automatic Segmentation of the Mandible From Limited-Angle Dental X-Ray Tomography Reconstructions*, From Nano to Macro, 2007, pp. 964–967.

37. P. Kamencay, M. Breznan, Roman Jarina, Martina, Zachariasova *Estimation and Image Segmentation of a Sparse Disparity Map for 3D Reconstruction*, Kamencay Proceedings Estimation AI, 2012.

38. H. Lamecker, S. Zachow, A. Wittmers, B. Weber, H. Hege, B. Elsholtz, M. Stiller, *Automatic segmentation of mandibles in low-dose CT-data*, Int. J. of Comp. Ass. Rad. Surg., 2006, p. 393.

39. D. Kainmueller, H. Lamecker, H. Seim, M. Zinser, S. Zachow, *Automatic Extraction of Mandibular Nerve and Bone from Cone-Beam CT Data*, Med Image Comput Comut Assist Interv, 2009, pp. 76–83.

40. I. Barandiaran, I. Maca, E. Berckmann, D. Wald, M. Dupillier, C. Paloc, M. Grana, *An automatic segmentation and reconstruction of mandibular structures from CT-data*, Proc. Int. Conf. on Intelligent Data Eng. and Automated Learning, 2009, pp. 649–655.

41. G. Tognola, M. Parazzini, G. Pedretti, P. Ravazzani, F. Grandori, A. Pesatori, M. Norgia, C. Svelto, *Novel 3D Reconstruction Method for Mandibular Distraction Planning*, (IST), International Workshop on Imaging Systems and Techniques Minori, 2006, pp. 3–6.

42. D. Kainmueller, H. Lamecker, H. Seim, S. Zachow, *Multi-object Segmentation of Head Bones*, MIDAS Journal, Contribution to MICCAI Workshop Head and Neck Auto-Segmentation Challenge, p. 1, 2009.

43. M. Mahoor, M. Abdelmottaleb, *Classification and numbering of teeth in dental bitewing images,* Pattern Recognition, 2005, pp. 577–586.

44. D. Nassar, A. Abaza, H. Ammar, *Automatic Construction of Dental Charts for Postmortem Identification*, IEEE Transactions on Information Forensics and Security, 2008, pp. 234–246.

45. P. Lin, Y. Lai, P. Huang, *An effective classification and numbering system for dental bitewing radiographs using teeth region and contour information*, Pattern Recognition, 2010, pp. 1380–1392.

46. H. Gao, O. Chae, *Automatic Tooth Region Separation for Dental CT Images,* Conf. on Conv. and Hybrid Inf. Tech., 2008, pp. 897–901.

47. M. Hosntalab, R. Aghaeizadeh Zoroo, A. Abbaspour Tehrani-Fard, G. Shirani, *Segmentation of teeth in CT volumetric dataset by panoramic projection and variational level set*, Int. J. of Comp. Ass. Rad. Surg., 2008, pp. 257–265.

48. I.B. Pavaloiu *et al.*, *3D Dental Reconstruction from CBCT Data*, Proceedings of the International Symposium on Fundamentals of Electrical Engineering, ISFEE, 2014.

49. I.B. Pavaloiu *et al.*, *Knowledge Based Segmentation for fast 3D Dental Reconstruction from CBCT*, Proceedings of International Conference of Control Systems and Computer Science (CSCS20), 2015, pp. 397–401.

50. I.B. Pavaloiu, N. Goga, I. Marin, A. Vasilateanu, *Automatic segmentation for 3D dental reconstruction*, Proceedings of IEEE 6th ICCCNT, pp. 216–221, 2015.

51. I. Marin, I.B. Pavaloiu, N. Goga, A. Vasilateanu, G. Dragoi, *Automatic Contour Detection from Dental CBCT DICOM Data*, Proceedings of IEEE e-Health and Bioengineering Conference (EHB), 2015.

52. I. B. Pavaloiu *et al.*, *Neural Network Based Edge Detection for CBCT Segmentation*, Proceedings of IEEE e-Health and Bioengineering (EHB), 2015.

53. I.B. Pavaloiu *et al.*, *Teeth Labeling from CBCT Data Using the Circular Hough Transform*, Proceedings of the International Symposium on Fundamentals of Electrical Engineering (ISFEE), 2016.

54. I. Marin, N. Goga, B. Păvăloiu, A. Vasilateanu, *AIMMS System Framework: Automatic Dental Pathologies Recognition from DICOM files*, 2nd Annual IEEE International Symposium on Systems Engineering (ISSE), 2016, pp. 81–85.

55. I.B. Pavaloiu, N. Goga, A. Vasilateanu, I. Marin, *3D Reconstruction from CBCT Data used in Dentistry Learning* (ICERI), the 9th annual International Conference of Education, Research and Innovation, 2016, pp. 5020–5029.

56. I. Marin, N. Goga, A.I Vasilateanu, I.B. Pavaloiu, *AIMMS – Integrated Platform for Extracting Dental Knowledge Imaging and 3D Modeling*, EHB, 2017.